Research Article | Vol. 32, No. 17 / 12 Aug 2024 / Optics Express 30898
Optics EXPRESS

Photonic sampling of microwave signals with adjustable sampling frequencies using an optical frequency comb

RUI YANG,[1] VALERIA VERCESI,[2] ALWYN SEEDS,[1] AND CHIN-PANG LIU[1]

[1]Department of Electronic & Electrical Engineering, University College London, Torrington Place, London WC1E 7JE, UK
[2]Università degli Studi di Pavia, Strada Nuova 65, 27100, Pavia, Italy

Abstract: We propose and demonstrate what we believe to be a novel photonic sampling technique using an agile optical frequency comb generator achieving flexible sampling frequencies. Several comb lines are carved into sampling pulses which are then time-dispersed along a single-mode optical fiber as a function of the electronically adjusted comb line spacing and the number of comb lines selected. Successful sampling and demodulation of QAM signals up to a 17 GHz carrier frequency with a sampling rate of up to 50 GSa/s have been demonstrated. A minimum of 1.5% EVM at 3 GHz and a maximum 4.4 bits (ENOB) at 2.1 GHz were also measured.

1. Introduction

Since the 1970s, photonic techniques have been introduced at the sampling stage to enhance the performance of electronic analog-to-digital converters (ADCs) [1–3], forming what is now generally termed the photonic ADC [4]. Benefitting from the low jitter levels of mode-locked lasers (MLLs) in optical pulse generation, photonic ADCs are increasingly seen to be able to overcome the bottleneck of electronic jitter. For example, the MLL employed in [5] generated an optical pulse train with an ultralow jitter of less than 10 fs for sampling microwave and millimeter-wave signals. Nowadays, research on photonic ADCs has achieved some inspiring results with the realization of the first entirely photonics-based radar system [6].

In the 1990s, researchers [7,8] proposed a discrete time-to-wavelength mapping by constructing a source with interleaved pulse trains of different wavelengths. Such wavelength- and time-interleaving techniques allow photonic ADCs to demultiplex a highspeed sampled pulse train into multiple low-rate, spectrally distinct pulse trains using a wavelength demultiplexer. In [9], a 2.1 GS/s photonic ADC implemented with two 1.05 GS/s time-interleaving channels was used to digitize a 41 GHz signal with 7.0 effective bits. In [10], an 18-wavelength pulse train was generated by spectrally slicing a 36.44 MHz MLL-generated optical comb and time-interleaved using a group of appropriate fiber delay lines, resulting in an 83.9 GS/s sampling clock signal. However, most MLL laser sources cannot readily allow their repetition rates to be adjusted and require constant stability adjustments, limiting their commercial exploitation outside laboratory environments.

Optical combs can also be generated using electro-optic modulators. Wu *et al.* [11] generated optical combs by modulating a CW laser with a cascade of lithium niobate intensity and phase modulators driven with specially tailored RF waveforms. Sakamoto *et al.* [12] theoretically proved that an asymmetrically driven dual-drive Mach-Zehnder modulator (MZM) could produce an optical comb with less than 3-dB ripples. Recently, such cavity-less comb sources have become increasingly popular in photonic ADC research. For example, in [13–15], two cascades

#532840 https://doi.org/10.1364/OE.532840
Journal © 2024 Received 17 Jun 2024; revised 4 Jul 2024; accepted 25 Jul 2024; published 9 Aug 2024

Optics EXPRESS

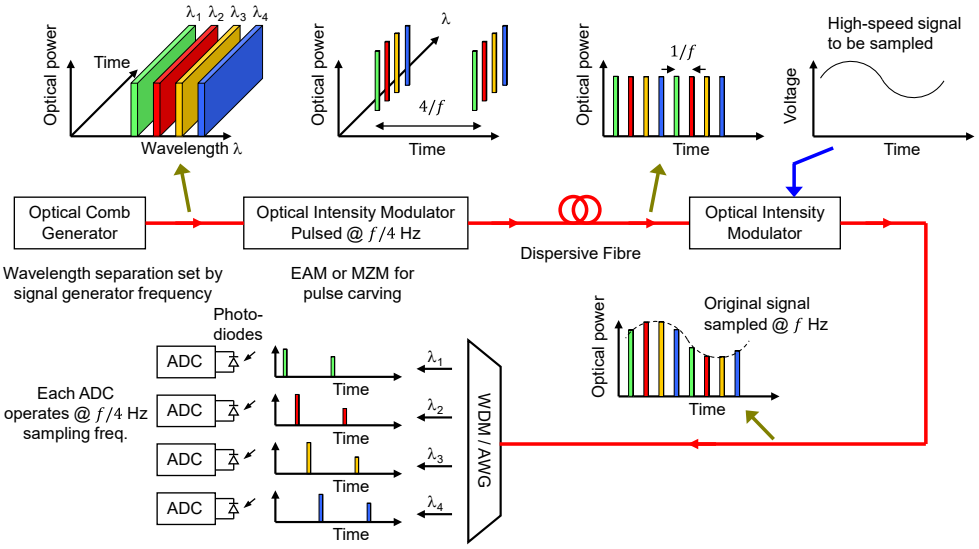

Fig. 1. The proposed photonic sampling technique based on an optical comb generator.

of intensity and phase modulators were respectively used to generate a 26 GHz sampling comb and a 27 GHz local oscillator comb to perform spectral slicing of a broadband RF signal. In [16–18], the cascades of MZMs or phase modulators also can be used to carve sinc-shaped optical pulse trains for sampling. Likewise, MZMs can be directly used as the cavity-less source of optical sampling pulses in other shapes, such as the Nyquist pulses [19,20].

In this paper, we propose and demonstrate a novel photonic sampling technique based on a frequency-agile optical comb. The optical comb is generated using a cascade of two electro-optic phase modulators which in turn are driven with a mm-wave signal generator whose output frequency also sets the comb line spacing. A MZM is then used to carve sampling pulses into each of the optical comb lines. Through the selection of up to 4 different optical comb lines and setting of the pulse carving frequency, flexible photonic sampling rates of up to 50 Ga/s have been achieved. We also report the signal-to-noise and distortion ratio (SINAD) results at different sampling rates and the successful sampling and demodulation of different QAM signals up to a 17 GHz carrier frequency.

2. Principle of the proposed photonic sampling

Figure 1 illustrates the schematic of our proposed photonic sampling technique. An optical comb can be generated by driving a combination of optical intensity or phase modulators with a microwave or mm-wave signal generator, whose adjustable output frequency determines the comb line spacing. An optical filter can then be used to select four equally spaced comb lines. These four comb lines are then carved into short optical pulses using an optical intensity modulator, such as an electroabsorption modulator (EAM) or an MZM, driven by another signal generator. The pulses at these four different wavelengths can be aligned uniformly along the time axis through a dispersive optical fiber, forming a pulse train with a repetition rate four times faster than the pulse carving frequency. Subsequently, the input RF analog signal can now be photonically sampled in another optical intensity modulator with this pulse train. Since the sampling pulse train is formed of four slower pulse trains of four different wavelengths, it can be demultiplexed, after signal sampling, into four different optical signals using a commercially available arrayed waveguide grating, a wavelength division demultiplexer or a WaveShaper. As a result, each

Optics EXPRESS

demultiplexed optical signal can be photo-detected and digitized using a conventional electronic ADC at a sampling frequency of, ideally, equal to one quarter of the overall sampling frequency.

The ability to adjust the signal sampling frequency in this technique stems from the fact that both the optical comb line spacing and the pulse carving frequency can be set simply by changing the output frequencies of the signal generators driving the corresponding modulators. The relationship between the comb line spacing and the pulse carving frequency is determined by the required sampling frequency, and the length and dispersion of the deployed dispersive fiber. Suppose the frequency spacing between any two neighboring selected comb lines is Δf, after transmission through the dispersive fiber, there will be a relative time delay $\Delta\tau$ between the two comb lines given by

$$\Delta\tau = D \cdot L \cdot \Delta\lambda = D \cdot L \cdot \left(-\frac{\lambda^2}{c} \cdot \Delta f\right) \tag{1}$$

where D and L are the dispersion coefficient and the length of the fiber, respectively, $\Delta\lambda$ and Δf are the comb line spacing in wavelength and frequency, λ is the center wavelength of the optical comb, and c is the speed of light. When the pulse trains are aligned uniformly in the time-domain, the signal sampling frequency f_s and $\Delta\tau$ are related by

$$\Delta\tau = \frac{1}{f_S} \tag{2}$$

and the number of comb lines used, N, links both f_s and the pulse carving frequency f_{PC} via

$$f_S = N \cdot f_{PC} \tag{3}$$

Finally, combining Eqs. (1), (2), and (3) yields

$$f_S = N \cdot f_{PC} = -\frac{c}{D \cdot L \cdot \lambda^2} \cdot \frac{1}{\Delta f} \tag{4}$$

For example, to establish a sampling frequency of 40 GSa/s, the comb generator can be driven at 40 GHz, and four alternate comb lines with 80 GHz spacing are then selected with a

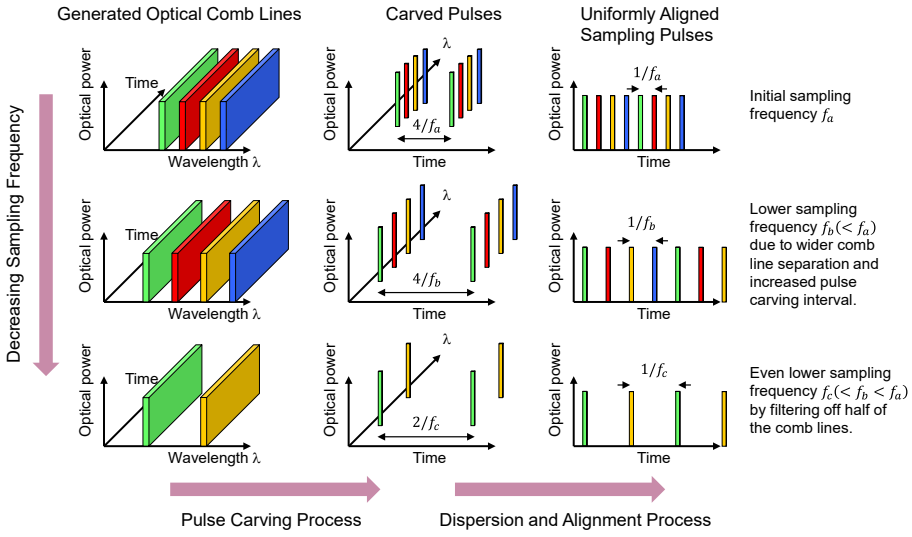

Fig. 2. Flexible sampling frequencies by adjusting comb line spacing, the pulse carving frequency, and/or the number of comb lines used.

Optics EXPRESS

WaveShaper. Using a standard single-mode fiber (SMF) as the dispersive fiber with $D = 16.85$ ps/(nm. km) and an input laser wavelength of 1550 nm, the required fiber length is calculated to be 2.316 km. On the other hand, it is appreciated that it would be difficult in practice to obtain such a precise length of fiber. Also, once a dispersive fiber has been chosen and deployed, it is not expected that it will be changed just because the sampling frequency needs to be adjusted. Instead, the sampling frequency is adjusted electronically by changing the comb line spacing, the pulse carving frequency, and the number of comb lines used according to Eq. (4). For example, the sampling frequency can be decreased by a combination of 1) decreasing the pulse carving frequency, 2) increasing the comb line spacing, and/or 3) decreasing the number of comb lines used, as illustrated in Fig. 2. A similar consideration applies to increasing the sampling frequency.

3. Experimental arrangement

A proof-of-concept experiment has been conducted to demonstrate how flexible sampling frequencies can be achieved for sampling microwave signals with this technique. Figure 3 shows the experimental arrangement.

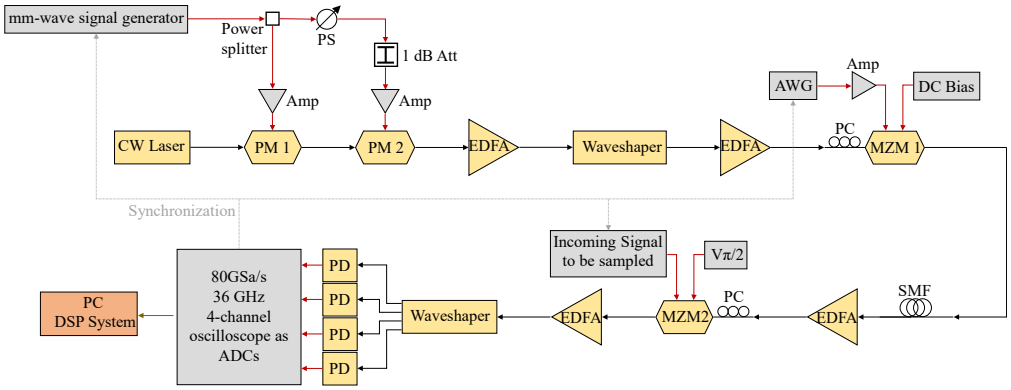

Fig. 3. Experimental arrangement. Amp: electrical amplifier; 1 dB Att: 1 dB electrical attenuator; PS: phase shifter; EDFA: Erbium-doped fiber amplifier; PC: polarization controller; MZM1,2: Mach Zehnder modulator; AWG: arbitrary waveform generator; SMF: standard single-mode fiber; PD: photodiode; DSP: digital signal processing.

A 1550 nm CW laser (IDPhotonics CoBrite DX1) of 15.5 dBm output power was inputted to the first of two cascaded phase modulators (iXblue MPZ-LN-40), which were all simultaneously driven with a mm-wave signal generator (Rohde & Schwarz SMP-04) initially at 40 GHz. A microwave splitter, two RF amplifiers, a 1-dB RF attenuator, and a phase shifter were used to amplify the signal power to the required levels of about 27 dBm and adjust the relative phase that each modulator received. This arrangement of phase modulators generated many comb lines, and the signal generator frequency directly set the comb lines spacing. Of the many generated comb lines, as shown in Fig. 4 (a), only the six lines (λ_{-3}, λ_{-2}, λ_{-1}, λ_1, λ_2, and λ_3) around the center of the comb were considered to have sufficient optical powers, and a programmable WaveShaper (WaveShaper 4000s) was employed to select the required number of comb lines according to the sampling frequency and equalize their powers. For example, if four lines are required, those lines at wavelengths λ_{-3}, λ_{-1}, λ_1, and λ_3 can be selected, as shown in Fig. 4 (b). On the other hand, if two lines are required, λ_{-2} and λ_2 with an increased spacing can be selected instead.

Four optical comb lines were first selected according to Fig. 4 (b) and subsequently carved into short optical pulses using the first Mach Zehnder modulator (MZM1). Although being driven with a 10 GHz sinewave, this MZM1 was not set up to create sinc-shaped pulses as in [16,17]; MZM1 was simply used as an intensity modulator to generate 10 GHz optical pulses of

Optics EXPRESS

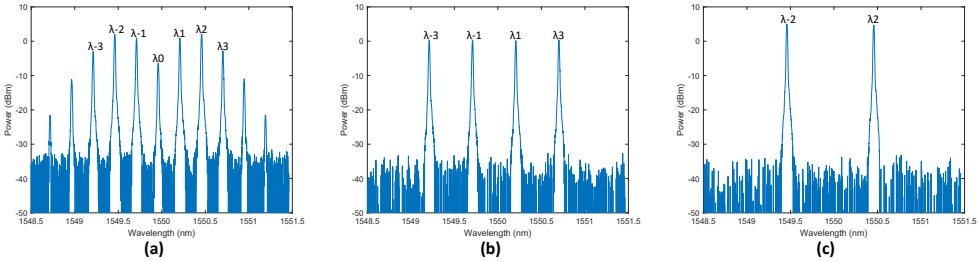

Fig. 4. (**a**) The optical spectra of the original comb with 40 GHz spacing, **(b)** the filtered 4-line comb with 80 GHz spacing, and **(c)** the filtered 2-line comb with 160 GHz spacing. Resolution bandwidths were 0.01 nm.

no particular shape, although the DC bias of MZM1 was manually adjusted between the null point and the quadrature point to obtain a good balance between the peak power and the width of the generated optical pulses.

A Keysight M8195A arbitrary waveform generator (AWG) was used to provide the 10 GHz sinewave to MZM1 and was selected purely for convenience. The AWG has a rms jitter of about 200 fs and in hindsight, a low jitter/phase noise microwave synthesizer could have been used.

With a 20.3 dBm, 10 GHz sinusoidal signal driving MZM1, this carving process produced four 10 GHz repetition rate pulse trains at the four selected comb line wavelengths, which all overlapped in the time domain. Figure 5 shows the photo-detected waveform of one of the four pulse trains after being filtered with an optical filter. To align the four pulse trains in the time domain in order to obtain a 40 GHz time-multiplexed pulse train, they were sent and dispersed through a standard single-mode fiber (SMF) of about 2.4 km with a dispersion coefficient of about 16.85 ps/(nm. km).

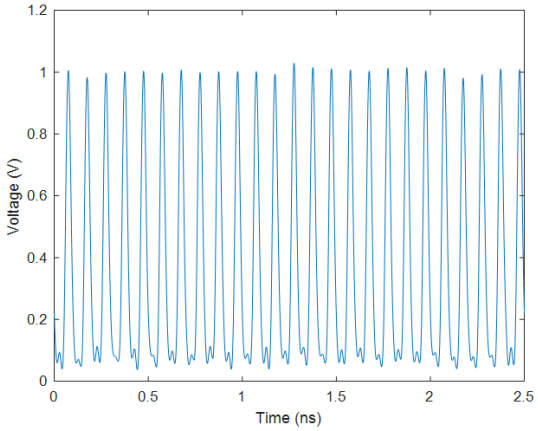

Fig. 5. The photodetected waveform of the 10 GHz optical sampling pulse train in one of the four channels from MZM1.

Since the exact length of the SMF was not precisely known, a separate measurement was carried out to determine the fiber length independently. A network analyzer, an MZM, and a photodiode were used to determine the relative group delay of a 1 GHz intensity-modulated sine wave transmitted over the said SMF as the wavelength of the CW input light to the MZM was varied. Having converted the CW light wavelength to optical frequency, the results are plotted in Fig. 6, from which a gradient of $\Delta\tau/\Delta f = 0.323$ ps/GHz is obtained.

Optics EXPRESS

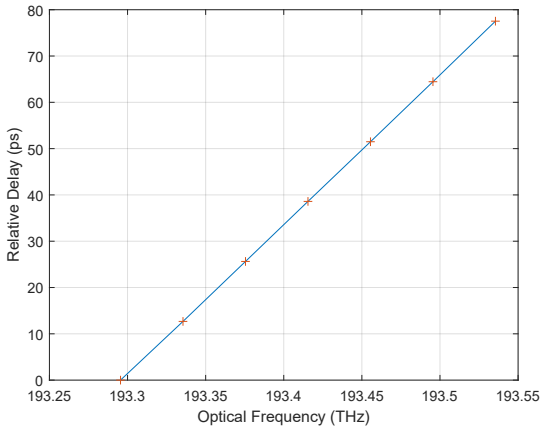

Fig. 6. The measured relative group delay versus optical frequency.

The fiber length is therefore calculated to be

$$L = \frac{\Delta\tau}{\Delta f} \cdot \frac{c}{\lambda^2 \cdot D} \approx 2.4 \text{ km} \tag{5}$$

which would then be used to re-calculate the required comb line spacings for the desired sampling frequency, as explained in the previous section. This 2.4 km fiber introduce a latency of about 12 μs. Therefore, to obtain a sampling frequency of 40 GSa/s from a 4-line comb with an inter-pulse interval of $\Delta\tau = 25$ ps, the required comb line space is calculated to be $\Delta f = 77.4$ GHz which can be obtained by driving the cascade of phase modulators at 38.7 GHz and selecting alternate comb lines as in Fig. 4 (b). These simple measurement with a network analyzer and calculation demonstrates that although the dispersive fiber length is fixed and often not known precisely, the amount of dispersion can be electronically tuned by adjusting the comb line spacings, resulting in flexible and accurate pulse alignment along the time axis. Compared to the pulse alignment using custom-designed phase shifters fabricated on a silicon platform in [16], our pulse alignment approach employs entirely commercial-off-the-shelf components and can therefore be modified readily, if necessary.

We performed photonic sampling on a 2 GHz sinewave. The 2 GHz analog input signal modulated the intensity of the optical sampling pulses traversing a second optical intensity modulator (MZM2) (IXBLUE MXAN-LN-40). Subsequently, pulse trains of different center wavelengths, whose intensity now carried the input analog RF signal, were demultiplexed using a second programmable WaveShaper (WaveShaper 4000s). As a result, each of the demultiplexed channels, with a power of around 3.5 dBm, was respectively detected with a broadband photodiode and then digitized at 80 GSa/s using one channel of a 4-channel real-time 36 GHz LeCroy oscilloscope acting as an ADC. Although the maximum pulse repetition rate used was only 15 GHz for sampling at 30 GSa/s, to fully demonstrate the waveform of sampled pulse trains and explain the adjusting mechanism of sampling frequency in this paper, an 80 GSa/s oscilloscope with 36 GHz input analog bandwidth was still configured to capture the input signals in this proof-of-concept experiment.

Finally, the captured waveforms from all the channels were transferred to a PC for further digital signal processing (DSP). All the initial channel waveforms were firstly oversampled to 200 times the pulse carving frequency. For example, if 10 GHz was chosen for the pulse carving frequency, the channel waveforms would be oversampled to 2 TSa/s. This oversampling process interpolates the channel waveforms and allows the algorithm to pick the sampled values more

Optics EXPRESS

accurately at the peaks of the optical sampling pulses. Subsequently, because the different optical paths would inevitably have slightly different paths and coupling losses as well as slightly different responsivities from the individual photodiodes, the different channels were mathematically scaled or normalized, which was based on the average optical power in each channel, and the corresponding photo-detected DC voltage measured by the oscilloscope. Finally, the original input RF signal was reconstructed according to the selected peak values after adjusting for channel path delays, as shown in Fig. 7.

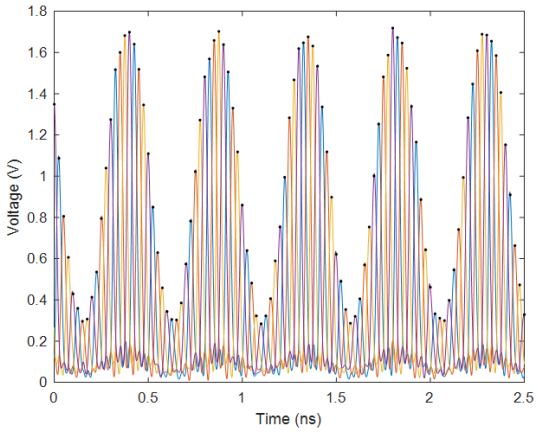

Fig. 7. The sampled 2 GHz input signal reconstructed from the four sampling pulse trains.

4. Experimental results

The constructed photonic ADC was first characterized in terms of the SINAD using sinusoidal inputs provided by a signal generator (Rohde & Schwarz SMF100A). Five different sampling frequencies were set according to the principle described in Section 2 and with their respective driving frequency, comb line spacing, pulse carving frequency, and the selected wavelengths, as shown in Table 1. For example, to set a 40 GS/s sampling frequency, the drive frequencies for the phase modulators and the pulse carving frequency were set at 38.7 GHz and 10 GHz, respectively. Four wavelengths, λ_{-3}, λ_{-1}, $\lambda_{1,}$ and λ_3, were selected by the first WaveShaper, giving a comb line spacing of 77.4 GHz between any two neighboring lines.

Table 1. The parameter settings for sampling frequencies of 20 GSa/s, 25 GSa/s, 30 GSa/s, 40 GSa/s, and 50 GSa/s.

Sampling Frequency	Driving Frequency	Comb Line Spacing	Pulse Carving Frequency	Selected Wavelengths
20 GSa/s	38.7 GHz	154.8 GHz	10 GHz	λ-2, λ2
25 GSa/s	31 GHz	124 GHz	12.5 GHz	λ-2, λ2
30 GSa/s	25.8 GHz	103.2 GHz	15 GHz	λ-2, λ2
40 GSa/s	38.7 GHz	77.4 GHz	10 GHz	λ-3, λ-1, λ1, λ3
50 GSa/s	31 GHz	62 GHz	12.5 GHz	λ-3, λ-1, λ1, λ3

The frequencies of the SINAD measurements started at 1.1 GHz and then increased in steps of 1 GHz. Also, the input signal power was 14 dBm at 1.1 GHz and progressively increased to around 20 dBm at high frequencies (>20 GHz) to compensate for an increase in Vpi and cable loss. Only those frequencies within the corresponding first Nyquist zone, as determined by the

Optics EXPRESS

set sampling frequency, were used. Once transferred to the PC, the SINADs of the reconstructed sine waves were calculated in LabVIEW. Figure 8(a) shows the spectrum of a 3.1 GHz sinusoidal signal sampled at 40 GSa/s from which a SINAD of 27 dB was measured. Figure 8(b) shows the measured SINAD curves vs. signal frequency at various sampling frequencies are shown in Fig. 8.

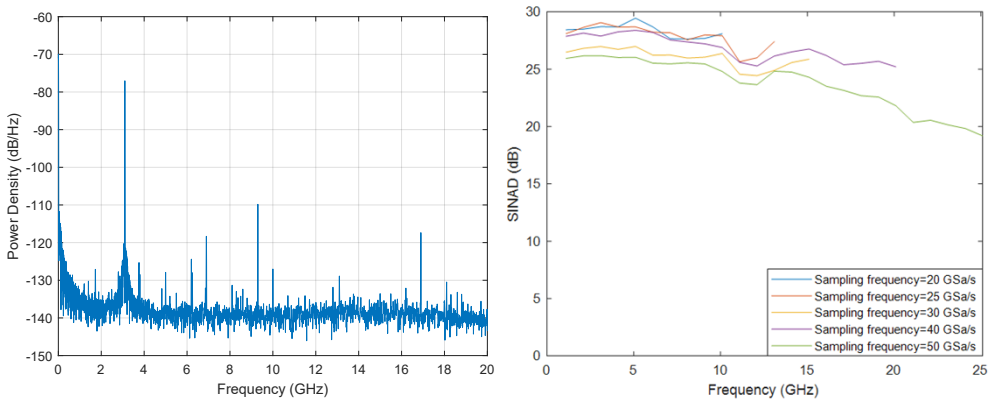

(a) (b)

Fig. 8. Measured SINADs. (a) Power spectral density of a 3.1 GHz sinusoidal signal sampled at 40 GSa/s from which a SINAD of 27 dB was measured. (b) Measured SINADs versus input signal frequency at sampling frequencies of 20 GS/s, 25 GS/s, 30 GS/s, 40 GS/s, and 50 GS/s.

At 20 GS/s, 25 GS/s, and 30 GS/s, the measured SINADs respectively remained above 27.6 dB (4.3 bits ENOB), 25.6 dB (4.0 bits), 24.4 dB (3.8 bits) for almost the entire measurement bandwidth. In these cases where only two comb lines participated in the sampling process, the significant factors limiting the system performance include the ASE noise produced by the employed optical amplifiers, the error in the signal peak selection by the algorithm and normalization process, and the noise and distortions from electronic ADCs. Moreover, the different frequency responses of RF amplifiers and pulse carving MZM, and the difference in optical bandwidths also caused a slight difference in the performances with different pulse

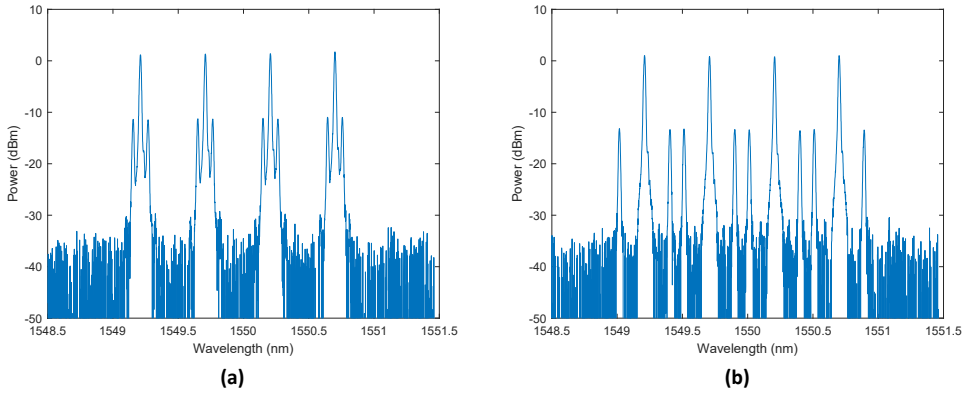

Fig. 9. Measured optical spectrum of the 4-line comb (at 50 GSa/s) being modulated by (a) a 7.1 GHz sinewave RF signal, (b) a 24.1 GHz sinewave RF signal. Resolution bandwidths are 0.01 nm.

Optics EXPRESS

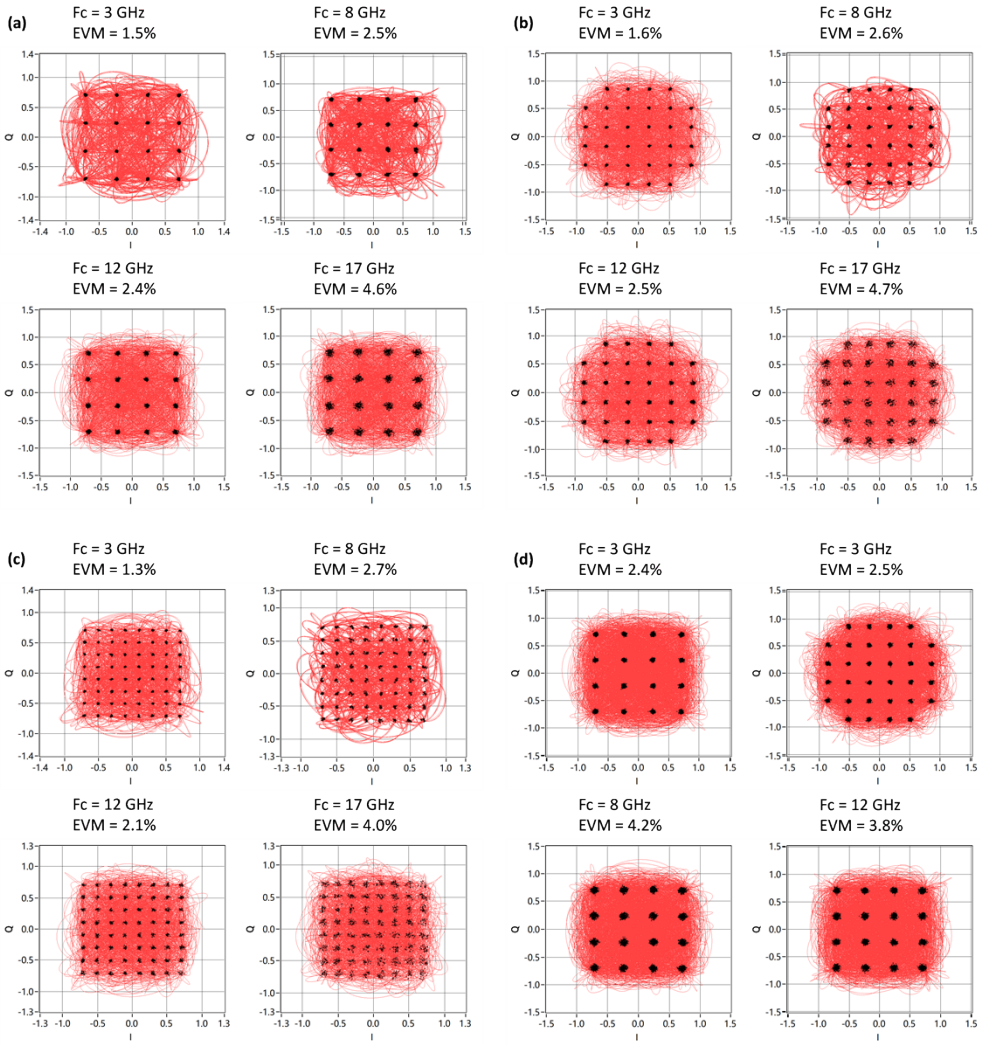

Fig. 10. Constellation diagrams and EVM values of (a) 1 Gbaud 16 QAM signals; (b) 1 Gbaud 32 QAM signals; (c) 1 Gbaud 64 QAM signals; (d) 2 Gbaud 16 and 32 QAM signals. Fc: Carrier frequency of the incoming QAM signals; EVM: Error vector magnitude; SR: Symbol rate.

carving frequencies. In addition, the 200-fs jitter of the AWG may also have contributed to the performance limitations. Using the 8.1 GHz sinusoidal signal sampled at 25 GSa/s as an example, the calculated jitter from the measured ENOB was 820 fs and therefore the AWG may have contributed about a quarter of the jitter to the sampled sinewave.

However, at 40 GS/s, the SINAD decreases slightly from 28.2 dB (4.4 bits) at 2.1 GHz to 25.7 dB (4.0 bits) at 19.1 GHz. Furthermore, it can be observed that the tendency of SINAD to decrease at 50 GS/s becomes more apparent (decreasing from 26.2 dB (4.1 bits) at 2.1 GHz to 19.8 dB (3.0 bits) at 24.1 GHz). The degradation of the system's performance was caused by the spectral overlap between every two adjacent channels. According to Eq. (4), to increase the sampling frequencies, this system needs to simultaneously increase its pulse carving frequency and decrease the comb line spacing, thereby causing a decrease in the spectral interval between

Optics EXPRESS

any adjacent channels. Therefore, with an increase in the frequency of signals to be sampled, in each channel, the sidebands of the sampled signal in one channel will increasingly overlap with those of adjacent channels. After being transformed to the RF domain by photodiodes, the distortions produced by the inter-channel spectral overlap will become complicated and difficult to compensate. To illustrate the distortions produced by the spectral overlap problem, Fig. 9 shows the optical spectra of the 4-line comb (62 GHz spacing for 50 GSa/s) only being modulated by a 7.1 GHz and a 24.1 GHz sinewave RF signal, respectively. To observe the difference in optical spectra more clearly, the optical pulse carver was switched off in this experiment. When sampling the higher frequency signals, the modulated spectral components will become closer to channel boundaries and even overlap with the neighboring channels, thus degrading the performance. Additionally, switching on the optical pulse carver will produce higher order modulated spectral components sampled by the pulse train, which will aggravate the spectral overlap distortion problem. One suggested solution to this problem is to select those comb lines which are further apart from each other. This would increase the spectral interval between them and hence decrease the overlap when they are modulated.

Finally, to evaluate sampling performance for broadband modulated microwave signals, we applied different QAM microwave signals to the system to be photonically sampled at 40 GSa/s and then demodulated. In this experiment, the different microwave QAM signals of carrier frequencies up to 17 GHz and symbol rates of up to 2 GBaud were generated by an AWG and then amplified to about 10.9 dBm by another RF amplifier (Mini-Circuits ZVA-213+) before modulating the dispersed optical pulse train traversing MZM2. Demodulation and analysis of the sampled QAM signals were performed in LabVIEW. The measured constellation diagrams and the corresponding error vector magnitude (EVM) values for 16-, 32- and 64-QAM signals of different carrier frequencies of 3, 8, 12, and 17 GHz at 1 or 2 GBaud are shown in Fig. 10. It can be seen that successful sampling, signal reconstruction and demodulation were achieved with these signal and sampling parameters. When sampling 1 Gbaud 16-, 32- and 64-QAM signals, the EVM performance of our system was measured to be below 1.6% at a low frequency of 3 GHz, below 2.7% at middle frequencies of 8 and 12 GHz, and below 4.7% at a high frequency of 17 GHz. The degradation of EVM performance could be attributed to the increased V_π of the MZM at increasing frequencies and the spectral overlapping problem mentioned earlier.

5. Conclusion

We proposed a photonic sampling technique with tunable sampling frequencies based on an agile optical comb and carved optical pulse trains, whose spacing and repetition rate can be electronically adjusted. We carried out photonic sampling of microwave sinusoidal signals and measured the SINADs at sampling frequencies of 20 GSa/s, 25 GSa/s, 30 GSa/s, 40 GSa/s, and 50 GSa/s. We further performed and successfully demonstrated sampling and demodulation of different microwave QAM signals up to 2 GBaud at 40 GSa/s using the proposed system.

Different from the photonic ADCs based on MLLs, our novel technique enables a highly flexible and electronic-controlled sampling rate and bandwidth as required. Additionally, our technique time-aligns the pulse trains of different wavelengths uniformly by using a 2.4 km SMF rather than multiple optical delay lines used in [9], minimising the timing error of interleaved sampling pulses.

The key factor limiting the performance of the proposed photonic sampling technique is the small comb line spacings achieved with the current electro-optic phase modulators. When these comb lines are modulated with a high-frequency microwave signal, the modulation sidebands of one comb line get close to those of other comb lines, making it difficult to separate them sufficiently with a WaveShaper. One possible solution to alleviate this problem is to use multiple CW tunable lasers instead of an RF-driven optical comb to generate widely spaced optical comb lines.

Optics EXPRESS

Finally, the proposed system has been demonstrated in a laboratory environment on an optical bench assembled using commercially-off-the-shelf components. To exploit the idea commercially, it would be useful to consider if this proposed technique could be implemented on a silicon platform. The main passive optical components include the electro-optic modulators, optical filters and the dispersive medium. These components have already been realized directly on silicon. On the other hand, the main active optical components are the laser diode and optical amplifiers. These active components can only be realized using direct bandgap III-V materials and therefore a hybrid III-V-on-silicon approach would be needed [21].

Funding. Engineering and Physical Sciences Research Council (EP/M021939/1).

Disclosures. The authors declare no conflicts of interest.

Data availability. Data underlying the results presented in this paper are not publicly available at this time but may be obtained from the authors upon reasonable request.

References

1. H. Taylor, "An optical analog-to-digital converter - Design and analysis," IEEE J. Quantum Electron. **15**(4), 210–216 (1979).
2. A. E. Siegman and D. J. Kuizenga, "Proposed method for measuring picosecond pulsewidths and pulse shapes in cw mode-locked lasers," IEEE J. Quantum Electron. **6**(4), 212–215 (1970).
3. F. J. Leonberger and P. Moulton, "High-speed InP optoelectronic switch," Appl. Phys. Lett. **35**(9), 712–714 (1979).
4. G. C. Valley, "Photonic analog-to-digital converters," Opt. Express **15**(5), 1955–1982 (2007).
5. J. Kim, M. J. Park, M. H. Perrott, *et al.*, "Photonic subsampling analog-to-digital conversion of microwave signals at 40-GHz with higher than 7-ENOB resolution," Opt. Express **16**(21), 16509–16515 (2008).
6. P. Ghelfi, F. Laghezza, F. Scotti, *et al.*, "A fully photonics-based coherent radar system," Nature **507**(7492), 341–345 (2014).
7. A. Yariv and R. G. M. P. Koumans, "Time interleaved optical sampling for ultra-high speed A/D conversion," Electron. Lett. **34**(21), 2012 (1998).
8. J. U. Kang and R. D. Esman, "Demonstration of time interweaved photonic four-channel WDM sampler for hybrid analogue-digital converter," Electron. Lett. **35**(1), 60–61 (1999).
9. A. Khilo, S. J. Spector, M. E. Grein, *et al.*, "Photonic ADC: overcoming the bottleneck of electronic jitter," Opt. Express **20**(4), 4454–4469 (2012).
10. G. Wu, S. Li, X. Li, *et al.*, "18 wavelengths 83.9Gs/s optical sampling clock for photonic A/D converters," Opt. Express **18**(20), 21162–21168 (2010).
11. R. Wu, V. R. Supradeepa, C. M. Long, *et al.*, "Generation of very flat optical frequency combs from continuous-wave lasers using cascaded intensity and phase modulators driven by tailored radio frequency waveforms," Opt. Lett. **35**(19), 3234–3236 (2010).
12. T. Sakamoto, T. Kawanishi, and M. Izutsu, "Asymptotic formalism for ultraflat optical frequency comb generation using a Mach-Zehnder modulator," Opt. Lett. **32**(11), 1515–1517 (2007).
13. C. Deakin and Z. Liu, "Dual frequency comb assisted analog-to-digital conversion," Opt. Lett. **45**(1), 173–176 (2020).
14. C. Deakin, T. Odedeyi, and Z. Liu, "Dual frequency comb photonic analog to digital conversion," *2020 IEEE Photonics Society Summer Topicals Meeting Series (SUM)*, 2020, pp. 1–2.
15. C. Deakin and Z. Liu, "Frequency interleaving dual comb photonic ADC with 7 bits ENOB up to 40 GHz," *2022 Conference on Lasers and Electro-Optics (CLEO), San Jose, CA, USA*, 2022, pp. 1–2.
16. A. Misra, C. Kress, K. Singh, *et al.*, "Integrated source-free all optical sampling with a sampling rate of up to three times the RF bandwidth of silicon photonic MZM," Opt. Express **27**(21), 29972–29984 (2019).
17. S. Preußler, G. R. Mehrpoor, and T. Schneider, "Frequency-time coherence for all-optical sampling without optical pulse source," Sci. Rep. **6**(1), 34500 (2016).
18. M. Soto, M. Alem, M. A. Shoaie, *et al.*, "Optical sinc-shaped Nyquist pulses of exceptional quality," Nat. Commun. **4**(1), 2898 (2013).
19. V. Vercesi, D. Onori, J. Davies, *et al.*, "Electronically synthesized Nyquist pulses for photonic sampling of microwave signals," Opt. Express **25**(23), 29249–29259 (2017).
20. V. Vercesi, D. Onori, J. Davies, *et al.*, "Photonic sampling of broadband QAM microwave signals exploiting interleaved optical nyquist pulses," *2018 Optical Fiber Communications Conference and Exposition (OFC)*, 2018, pp. 1–3.
21. K. Van Gasse, R. Wang, and G. Roelkens, "27 dB gain III–V-on-silicon semiconductor optical amplifier with > 17 dBm output power," Opt. Express **27**(1), 293–302 (2019).